Surface-Wave Effects on Dielectric Sheathed Phased Arrays of Rectangular Waveguides

By C. P. WU AND V. GALINDO

(Manuscript received September 12, 1967)

A further study of the effects of dielectric slabs on the radiation characteristics of an infinite array of rectangular waveguides has been carried out. It is found that, in addition to causing substantial and sometimes beneficial changes in the array performance, the presence of dielectric slabs can give rise to sharp resonant peaks in the reflection coefficient at certain scan angles. The occurrence of such resonant peaks at which total reflection occurs is contingent upon the presence of space harmonics which have surface-wavelike field distribution. Extensive data for both the H and E planes of scan, when the array is covered with a single slab, have been obtained and are presented here. This paper discusses the influence of the dielectric constant, slab thickness, and waveguide wall thickness on the resonant peak location, and points out the relationship between the resonance phenomenon and the surface wave propagation over a corrugated surface. It also presents some further results for the thin sheath and their extension to multiple sheaths.

I. INTRODUCTION

We presented the radiation properties of a dielectric-loaded rectangular waveguide array in some detail in a previous paper[1] for two planes of scanning: the H plane and a quasi-E plane. (See Fig. 1.) We discussed the effects of a thick dielectric sheath placed inside or outside the array aperture. We concluded that the presence of a dielectric material can cause a substantial change in the array performance, so that dielectric material should be considered an integral part of the array when it is designed. Moreover, we demonstrated that the effects of a dielectric may be used to improve the match performance of an array, perhaps at the cost of a larger frequency sensitivity, by a judicious choice of the added physical parameters.

This paper deals with some different aspects of the problem based

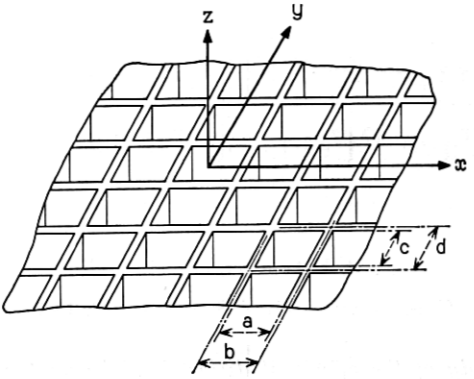

Fig. 1 — An infinite array of rectangular waveguides.

on an extensive further analysis. We completely removed the restrictions placed on the parameters in the previous work in order to analyze the full effects of a dielectric medium. In particular, since dielectric slabs can support surface waves, we direct special attention toward investigating the possibility of anomalous array behavior when dielectric slabs are used to cover the array. Indeed, a resonance phenomenon is found to exist due to the presence of trapped- (or surface-) wave type space harmonics at the air-dielectric interface. One important effect of such space harmonics is to cause the appearance of sharp resonant peaks in the reflection coefficient at certain scan angles. The peaks attain, for all practical purposes, values of unity. We present results for a dielectric slab of arbitrary thickness placed over an array, thereby, removing the previous restriction to thick slabs. We also discuss radiation through a stratified medium.

II. ANALYSIS

The approach we use in this work, as in previous ones,[1, 2] is based on an integral equation having either the aperture electric or the aperture magnetic field as the unknown function. One of the advantages of such an approach is that the integral equation may be easily and *rigorously* derived without any limitations from the physical parameters of the problems, and the approach is readily adaptable to a more general class of problems such as, for example, an array covered by a stratified dielectric medium. Although the basic procedures for formulating the integral equation have been discussed else-

where,[2, 11] in order to facilitate a further discussion of the formulation and to make this paper more or less self-contained, we present a brief derivation here and point out the modifications necessary for an extension to a more general situation of stratified media.

2.1 *Integral Equation Formulation of the Problem*

The procedure in the integral equation method is first to expand the fields into the appropriate normal modes in the various regions and then to match the boundary conditions across the interfaces. Consider, for example, an infinite array of parallel plates, covered with a single dielectric slab and scanned in the H plane as shown in Fig. 2. It is convenient in this case to divide the space into three regions, the region inside the waveguides, the region inside the dielectric slab, and the free space region. However, as will become evident shortly, it turns out that the geometry of the problem is such that it suffices to partition the space into two regions, inside and outside the waveguides.

The orthonormal modal functions and the modal impedances pertinent to the waveguide region are the usual ones given by

$$\varphi_n(x) = \begin{cases} \sqrt{\frac{2}{a}} \cos\left(\frac{n\pi}{a} x\right) \left(n = \begin{matrix}\text{odd} \\ \text{even}\end{matrix}\right) & \text{for } |x| \leqq \frac{a}{2} \\ 0 & \frac{a}{2} \leqq |x| \leqq \frac{b}{2} \end{cases}$$

and

$$Z_n = \omega\mu/\alpha_n$$

where

$$\alpha_n = \sqrt{k^2\epsilon_1 - \left(\frac{n\pi}{a}\right)^2}$$

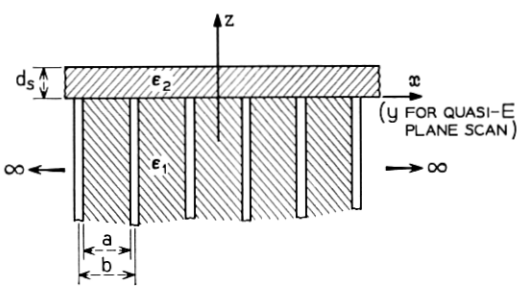

Fig. 2 — A parallel plate array covered by a dielectric sheath.

are the z-directed propagation constants for a waveguide filled with a dielectric of dielectric constant ϵ_1.

By using the Floquet theorem, it can be easily shown that the dielectric slab and free space regions have identical modal functions, owing to the requirement that the tangential fields must be continuous at all points across the dielectric-free space interface. The normalized modal functions take the usual form:

$$\psi_m(x) = \sqrt{\frac{1}{b}}\, e^{j((2m\pi/b)+T_x)x}, \qquad m = 0, \pm 1, \cdots$$

where T_x is the phase shift per unit length. The modal impedances for these two regions are different, however. They are given respectively by

$$Z_m^D = \omega\mu/\beta_m\,, \qquad \beta_m = \sqrt{k^2\epsilon_2 - \left(\frac{2m\pi}{b} + T_x\right)^2}$$

for the dielectric region, $0 \leqq z \leqq d_s$, and

$$Z_m^0 = \omega\mu/\gamma_m\,, \qquad \gamma_m = \sqrt{k^2 - \left(\frac{2m\pi}{b} + T_x\right)^2}$$

for the free space, $d_s < z$.

When the fields in the various regions are expanded into the normal modes under the situation in which the waveguides are excited in the fundamental mode of unit amplitude, we have

$$\mathcal{H}_x(x, z) = \begin{cases} (e^{j\alpha_1 z} + Re^{-j\alpha_1 z})\varphi_1(x) + \sum_{n=2}^{\infty} I_n\varphi_n(x)e^{-j\alpha_n z} & z \leqq 0 \\ \sum_{m=-\infty}^{\infty} (I_m^+ e^{j\beta_m z} + I_m^- e^{-j\beta_m z})\psi_m(x) & 0 \leqq z \leqq d_s \\ \sum_{m=-\infty}^{\infty} I_m'\psi_m(x)e^{j\gamma_m(z-d_s)} & d_s \leqq z \end{cases}$$

$$\mathcal{E}_y(x, y) = \begin{cases} -Z_1(e^{j\alpha_1 z} - Re^{-j\alpha_1 z})\varphi_1(x) + \sum_{n=2}^{\infty} Z_n I_n\varphi_n(x)e^{-j\alpha_n z} & z \leqq 0 \\ -\sum_{m=-\infty}^{\infty} Z_m^D(I_m^+ e^{j\beta_m z} - I_m^- e^{-j\beta_m z})\psi_m(x) & 0 \leqq z \leqq d_s\,. \\ -\sum_{m=-\infty}^{\infty} Z_m I_m'\psi_m(x)e^{j\gamma_m(z-d_s)} & d_s \leqq z \end{cases} \tag{1}$$

A time convention of exp $(-j\omega t)$ is assumed and suppressed for brevity throughout this paper. The I's are the unknown modal coefficients. Waves of all modes travelling in both the positive and negative z directions are included in the fields for $0 \leqq z \leqq d_s$, because this region is situated between two interfaces. Likewise, the fields for $z \leqq 0$ contain waves travelling in the negative z direction due to the scattering at the array aperture.

We find, by applying the boundary conditions at $z = 0$, that

$$\begin{aligned} H_x(x) = \mathcal{H}_x(x, 0) &= (1 + R)\varphi_1(x) + \sum_{n=2}^{\infty} I_n\varphi_n(x) \\ &= \sum_{m=-\infty}^{\infty} (I_m^+ + I_m^-)\psi_m(x) \\ E_y(x) = \mathcal{E}_y(x, 0) &= -Z_1(1 - R)\varphi_1(x) + \sum_{n=2}^{\infty} Z_n I_n\varphi_n(x) \\ &= -\sum_{m=-\infty}^{\infty} Z_m^D(I_m^+ - I_m^-)\psi_m(x). \end{aligned} \tag{2}$$

Hence, on account of the orthonormality among the modal functions, it follows that

$$\begin{aligned} (1 + R) &= \int_{-b/2}^{b/2} \varphi_1(x)H_x(x)\, dx, \quad I_n = \int_{-b/2}^{b/2} \varphi_n(x)H_x(x)\, dx, \quad n \geqq 2 \\ I_m^+ + I_m^- &= \int_{-b/2}^{b/2} \psi_m^*(x)H_x(x)\, dx. \end{aligned} \tag{3}$$

Similarly, from the boundary conditions at the interface $z = d_s$,

$$\begin{aligned} \mathcal{H}_x(x, d_s) &= \sum_{m=-\infty}^{\infty} (I_m^+ e^{j\beta_m d_s} + I_m^- e^{-j\beta_m d_s})\psi_m(x) = \sum_{m=-\infty}^{\infty} I'_m\psi_m(x) \\ \mathcal{E}_y(x, d_s) &= -\sum_{m=-\infty}^{\infty} Z_m^D(I_m^+ e^{j\beta_m d_s} - I_m^- e^{-j\beta_m d_s})\psi_m(x) \\ &= -\sum_{m=-\infty}^{\infty} Z_m^0 I'_m\psi_m(x). \end{aligned} \tag{4}$$

By observing that the right and left sides of (4) are the field expansions with respect to the same set of modal functions, one may immediately write

$$\begin{aligned} I_m^+ e^{j\beta_m d_s} + I_m^- e^{-j\beta_m d_s} &= I'_m \\ Z_m^D(I_m^+ e^{j\beta_m d_s} - I_m^- e^{-j\beta_m d_s}) &= Z_m^0 I'_m\,. \end{aligned} \tag{5}$$

Equations (5) show that the air-dielectric interface at $z = d_s$ is a simple one in that the m^{th} order mode in the dielectric region couples

only into the same order mode in the free space region and vice versa. The implication of this result is that the fields at the air-dielectric interface are completely determined when the fields at the array aperture are obtained. Therefore, it is necessary only to solve for the aperture field alone. With this in mind, we may then make use of (2), (3) and (5) to derive an integral equation having only the aperture magnetic field as the unknown function. Thus,

$$2Z_1\varphi_1(x) = \int_{-b/2}^{b/2} \left\{ \sum_{n=1}^{\infty} Z_n\varphi_n(x)\varphi_n(x') + \sum_{m=-\infty}^{\infty} Z'_m\psi_m(x)\psi_m^*(x') \right\} H_x(x')\, dx' \tag{6}$$

where

$$Z'_m = Z_m^D \frac{Z_m^0 - jZ_m^D \tan \beta_m d_s}{Z_m^D - jZ_m^0 \tan \beta_m d_s}. \tag{7}$$

It is clear from expression (7) that the equivalent impedances Z'_m for the m^{th} order modes are the familiar input impedance of a transmission line, which has a characteristic impedance Z_m^D, propagation constant β_m, and length d_s, and is terminated in a load impedance Z_m^0. Notice also that only quantities pertaining to the m^{th} space harmonic appear in (7). All these facts suggest that the space exterior to the waveguides may be treated as a single region from the onset, as observed earlier, provided that the effects of the dielectric slab are taken into account through the use of appropriate modal impedances. Moreover, the integral equation given by (6) is readily extended to a more general situation in which the array is covered or loaded with stratified dielectric media (or both covered and loaded). Only the modal impedances need to be modified for this purpose.

As an example, suppose we wish to study the properties of an array covered by a stratified medium as Fig. 3 shows. Equation (6) still is a valid integral equation to use. In this case, the Z_n are the usual waveguide modal impedances, whereas the Z'_m are the modal impedances as seen at the array aperture of the N layer stratified dielectric medium, which may be calculated by standard techniques.[3]

The integral equation appropriate to the quasi-E plane of scan may be derived in a similar manner. In a quasi-E plane of scan, the scanning takes place in the plane of the electric field while there is a sinusoidal field variation in the direction normal to the plane of scanning.*

*Such a mode of scanning results from a planar array of rectangular waveguides, which is scanned in the E plane direction with a fixed scan angle of 180° applied in the H plane direction. This special scan case is considered for the sake of simplifying the problem. See Ref. 4.

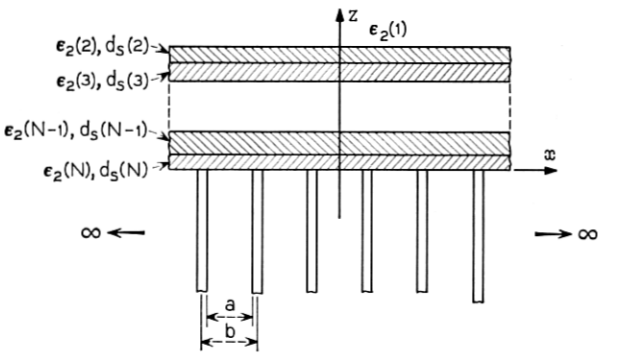

Fig. 3 — Radiation of an array through N dielectric sheaths.

The exterior modal functions for the quasi-E plane scan are the same as those for H plane scan, according to the Floquet theorem, but the wave modes which the waveguides support are different. The orthonormal modal functions for this case are

$$\omega_n(y) = \begin{cases} -\sqrt{\frac{\epsilon_n}{c}} \cos\left(\frac{n\pi}{c} y\right), & n = \begin{matrix}\text{even}\\ \text{odd}\end{matrix} \quad \text{for} \quad y \leqq \frac{c}{2} \\ 0 & \text{for} \quad \frac{c}{2} \leqq y \leqq \frac{d}{2} \end{cases}$$

Here we have used c for the internal waveguide width and d for the element spacing. A sinusoidal variation of $\sin[(\pi/b)x]$, which applies to all tangential field components, is omitted for brevity.

The integral equation with the aperture electric field as the unknown is given by

$$2Y_0\omega_0(y) = \int_{-c/2}^{c/2} \left\{ \sum_{n=0}^{\infty} Y_n\omega_n(y)\omega_n(y') + \sum_{-\infty}^{\infty} Y'_m\psi_m(y)\psi_m^*(y') \right\} E_y(y')\, dy',$$

where the

$$Y_n = \left[k^2\epsilon_1 - \left(\frac{\pi}{b}\right)^2 \right] \Big/ \omega\mu\alpha_n$$

are the interior modal admittances and the Y'_m are the exterior modal admittances with the presence of dielectric slab(s) appropriately taken into account.

2.2 *Method of Solution*

The method used in solving the integral equations is basically that of Galerkin,[5, 6] the method of moments. Briefly, in this method, the

first step is to expand the unknown function as a linear combination of N linearly independent functions. Substitution of the representation into the original integral equation leads to an approximate equation. The difference between the left and right sides of the approximate equation is then required to be orthogonal to the set of functions individually, thus yielding a set of N equations in N unknowns. The resulting set of equations may then be inverted with the help of an electronic computer.

There are different sets of functions one may choose to use in this approach. Although the choice, aside from consideration of computer time and convenience, seems to be largely a matter of personal preference, it is desirable to incorporate as much prior knowledge about the problem as possible. We have used the set of first N modal functions to obtain most of the results reported here. This step is tantamount to assuming the higher order modal coefficients to be zero. For example, to solve (6), we set

$$H_x(x) \approx \sum_{m=-M}^{M} \tilde{I}'_m \psi_m(x), \qquad \tilde{I}'_m = 0 \qquad |\, m \,| > M. \tag{8}$$

Substituting (8) into (6) leads to

$$2Z_1\varphi_1(x) - \sum_{m=-M}^{M} \left\{ \sum_{n=1}^{\infty} Z_n C_{nm} \varphi_n(x) + Z'_m \psi_m(x) \right\} \tilde{I}'_m \approx 0, \tag{9}$$

where

$$C_{nm} = \int_{-b/2}^{b/2} \varphi_n(x) \psi_m(x)\, dx.$$

The expression (9) is then required to be orthogonal to the set of functions $\psi_l^*(x)$, $l = 0, \pm 1, \cdots, \pm M$, individually, thus yielding

$$\sum_{m=-M}^{M} \left\{ \sum_{n=1}^{\infty} Z_n C_{nm} C_{nl}^* + Z'_m \delta_{ml} \right\} \tilde{I}'_m = 2Z_1 C_{1l}^* \quad l = 0, \pm 1, \cdots, \pm M. \tag{10}$$

The set of equations (10) may be solved by a standard technique. The reflection coefficient R is then obtainable from

$$(1 + R) = I_1 \approx \sum_{-M}^{M} C_{1m} \tilde{I}'_m \,. \tag{11}$$

Since it appears that there is no convenient scheme for estimating the error in the type of problem being considered here, the following procedures have been used to ascertain the accuracy of the results. They include:

(*i*) Observing the "convergence" of the solution by increasing N, the number of functions used to represent the unknown aperture field.

(*ii*) Using different sets of functions, such as the set of piecewise constant or pulse functions for the approximation.

(*iii*) Comparing the results with known solutions obtained by different methods where applicable.[4, 7, 8]

(*iv*) Applying the variational principle to check the adequacy of the algorithm used in the numerical procedure.

(*v*) Checking how well energy is conserved.

III. RESULTS

In the previous report,[1] we placed the emphasis on the results for the situations where the waveguides are either completely filled with a dielectric material or loaded with a dielectric slab. We also discussed some preliminary results for covering the array with a dielectric sheath. We obtained that data for a range of parameters such that, at most, one propagating mode could exist inside the dielectric region, and only relatively thick slabs were considered. Such a choice of the parameters was necessary in order that an approximation based on the transmission line theory could be applied.

The results presented here are concerned largely with the effects of dielectric sheaths covering the array. In particular, we concentrate on the situation in which more than one wave can propagate inside the dielectric region so that there will be trapped- (or surface-) wave-like space harmonics at the air-dielectric interface. Although in principle it is still possible in such cases to apply a *generalized* transmission line approximation, this approach might not be very convenient in practice. The modification required for generalization depends on the number of modes which can propagate inside the dielectric, and this number is, in turn, dependent on the dielectric constant being used. Moreover, the minimum slab thickness necessary for a valid approximate calculation might sometimes become so large that it would exclude a useful range of practical interest. Therefore, it is desirable to proceed with the solution of the appropriate integral equations without introducing any intermediate steps. Thus, the effects of the air-dielectric interface at $z = d_s$ on *all* the modes generated at the array aperture may be fully taken into account. By doing so, we are also able to obtain data for comparison with those calculated by using the transmission line theory, and thus gain a

general feeling for the accuracy of this type of approximation. Some results of such a comparison are presented in Ref. 1.

3.1 *General Remarks*

The effect of an ordinary dielectric ($\epsilon > 1$) on wave propagation is to slow down the phase velocity, or equivalently to shorten the wavelength. Hence, when a dielectric slab is placed over a phased array, two apparent element spacings (in terms of the wavelength) have to be considered: one inside the dielectric medium and the other in the free space; the former always greater than the latter. A difference in the element spacings as seen in the two regions results in different scan angles for the appearance or disappearnce of grating lobes in the respective regions. Consequently, when the fields are expanded into normal modes according to the Floquet theorem, there will be a range of scan angles over which the number of propagating modes inside the dielectric is larger than that in free space. A mode is said to be propagating when the corresponding z-directed propagation constant is real. In a linear array, this propagation constant is given by

$$\beta_m = \sqrt{k_0^2\epsilon - \left(\frac{2m\pi}{b} + T_x\right)^2},$$

with an appropriate ϵ for each region. It is easy to show that for $m < b/\lambda_\epsilon < (m + 1/2)$, where m is an integer and λ_ϵ is the wavelength of a plane wave in a medium with dielectric constant ϵ, the number of propagating modes will change from $(2m+1)$ for $0 \leqq T_x b < 2\pi(b/\lambda_\epsilon - m)$ to $(2m)$ for $2\pi(b/\lambda_\epsilon - m) \leqq T_x b \leqq \pi$. On the other hand, when $(m + 1/2) < b/\lambda_\epsilon < (m + 1)$, the number of propagating modes will increase by one from $(2m + 1)$ to $(2m + 2)$, when the scan angle passes from $0 < T_x b < 2\pi(m + 1 - b/\lambda_\epsilon)$ to $2\pi(m + 1 - b/\lambda_\epsilon) < T_x b < \pi$.

The wave modes which are propagating inside the dielectric and are evanescent in free space have the same field distribution as that of a surface wave. Such wave modes have profound effects on the radiation characteristics of a phased array as we will see in the examples. It is important to emphasize that a single wave mode of this type alone is *not* sufficient to satisfy the boundary conditions. In other words, all the modes are required to constitute a correct solution.

3.2 *H-Plane Scan Results*

Figs. 4 and 5 give the reflection coefficients as a function of scan for an infinite array of rectangular waveguides covered with a single

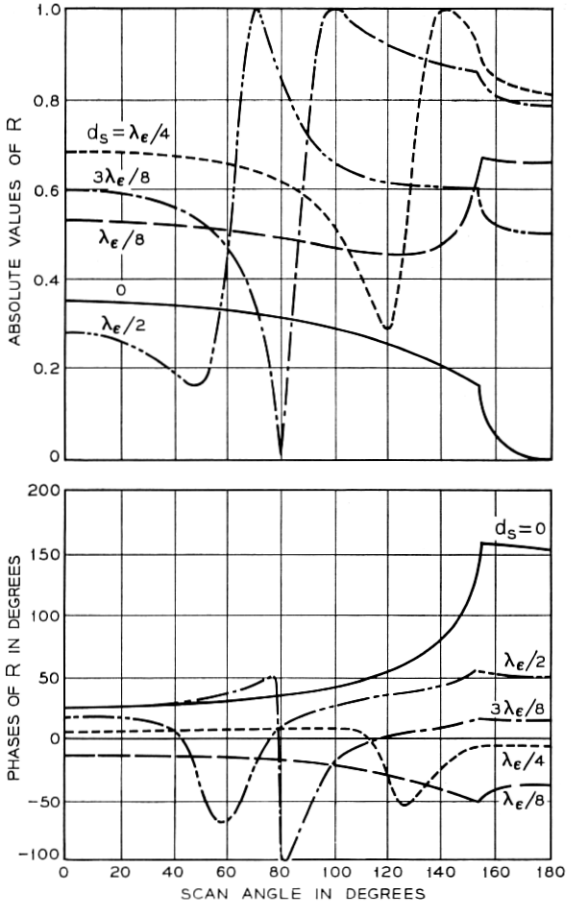

Fig. 4 — Reflection coefficient R vs scan angle $T_x b$ for H plane scan with $a/\lambda = b/\lambda = 0.5714$, and $\epsilon = 3.0625$.

dielectric sheath and scanned in the H plane. The results are obtained for the following parameters: $b/\lambda = a/\lambda = 0.5714$, $\epsilon = 3.0625$ with the thickness of the dielectric slab d_s varied over one λ_ϵ at an increment of $\lambda_\epsilon/8$, where λ_ϵ is the wavelength of a plane wave in the dielectric medium. Notice that the element spacing is measured in terms of the free space wavelength λ, for b/λ is the quantity which determines the number of radiated beams at a certain scan angle. With the given arrangement, the element spacing is such that the array radiates one beam for $0 \leqq T_x b \leqq 2\pi(1 - b/\lambda) = 154°$, and two beams when $2\pi(1 - b/\lambda) \leqq T_x b \leqq$

180°. The dielectric constant of the slab makes the apparent element spacing in the medium to be $b/\lambda_\epsilon = 1$. Thus, there are always two propagating modes inside the dielectric slab for all scan angles. As a result, we have in $0 \leqq T_x b \leqq 2\pi(1 - b/\lambda)$ a mode which exhibits a surface-wavelike behavior by being propagated inside the dielectric and evanescent in free space. The effect of such a mode is to cause the appearance of sharp resonant peaks in the reflection coefficient at certain scan angles as is evident from the graphs.

Based on the results presented here and some further calculations at different wavelengths, we may make the following general observations:

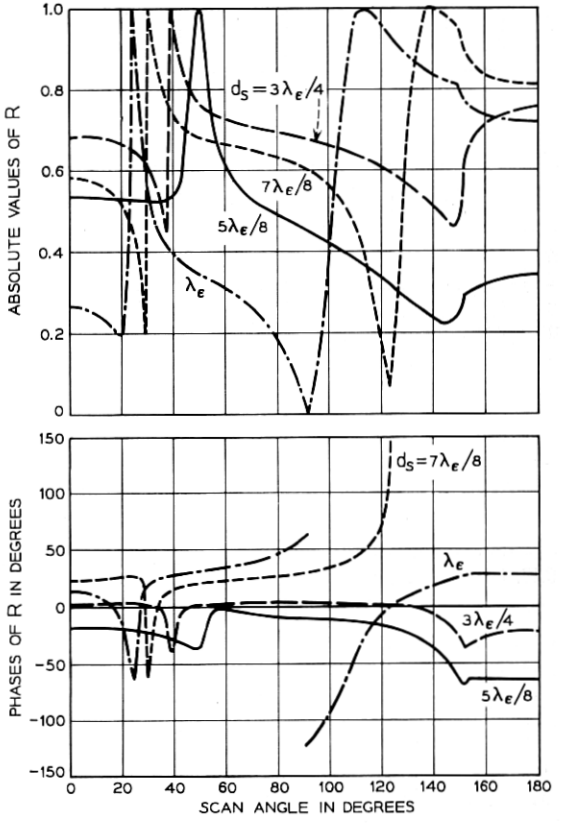

Fig. 5 — Reflection coefficient R vs scan angle $T_x b$ for H plane scan with $a/\lambda = b/\lambda = 0.5714$, and $\epsilon = 3.0625$.

(*i*) When the thickness of the dielectric slab is relatively small, no resonant peak occurs.

(*ii*) When the thickness is increased beyond a critical value, usually in the neighborhood of $3\lambda_\epsilon/16$, a resonant peak starts to appear at a scan angle close to the value $2\pi(1-b/\lambda)$, and the peak is usually preceded by a dip.

(*iii*) Increasing the slab thickness causes the peak to move toward the broadside direction and the peak becomes sharper.

(*iv*) A further increase in the slab thickness makes more than one peak appear.

(*v*) The peaks attain, for all practical purposes, values of unity.

The dielectric constant used in obtaining the results for Figs. 4 and 5 was chosen to have a value $\epsilon = (\lambda/b)^2$. This creates a situation where one space harmonic possesses a surface-wavelike field distribution in $0 \leqq T_z b \leqq 2\pi(1 - b/\lambda)$. It is possible for a resonant peak to appear at any scan angle within this range. If a smaller dielectric constant had been used, the range of scanning over which a resonant peak might appear would be reduced accordingly. On the other hand, a larger value of dielectric constant would give rise to more than one surface-wavelike space harmonic, and it is possible for resonant peaks to appear with dielectric slab of thickness even smaller than $3\lambda_\epsilon/16$.

Recall that when we use a dielectric slab of small dielectric constant and large slab thickness, the transmission line approximation may be effectively applied to yield useful results.[1] The reflection coefficients calculated under such conditions are periodic functions of the slab thickness; hence, the calculations only need be performed over a period, that is, a half guided wavelength. If the dielectric constant is large so as to permit more than one propagating mode inside the dielectric, however, the periodic property is no longer present, and separate calculations have to be carried out for different slab thicknesses.

Fig. 6 is typical of the transmission coefficients calculated for $b/\lambda = a/\lambda = 0.5714$, $\epsilon = 3.0625$ and $d_s = \lambda_\epsilon/2$. These transmission coefficients are referred to the air-dielectric interface $z = d_s$. The figure shows both the transmission coefficients for the zeroth order mode (corresponding to the main beam) and the first space harmonic (corresponding to a grating lobe). These coefficients are defined so that the sum of the reflection coefficient squared and the square of the transmission coefficient(s) equals one. Thus, if T_0 and T_1 denote the

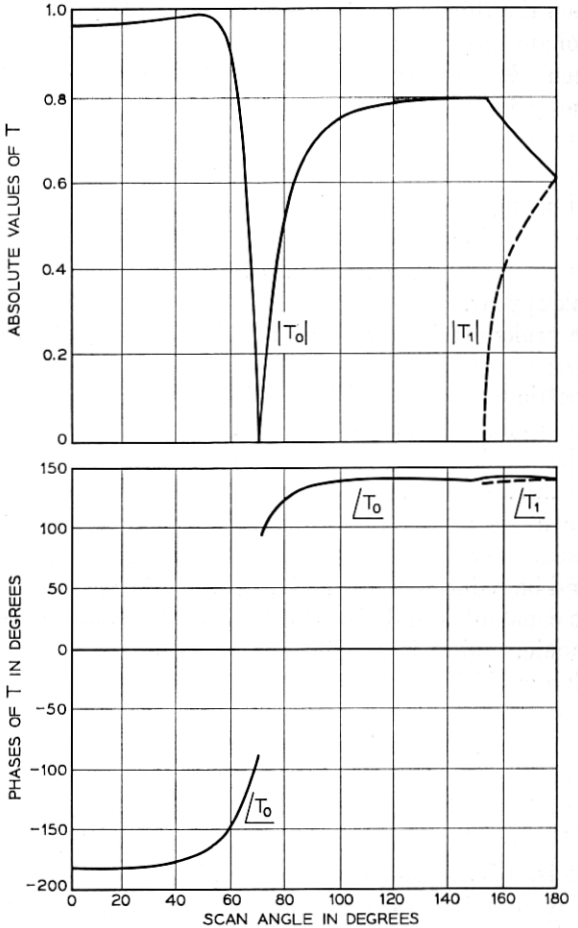

Fig. 6 — Transmission coefficients T vs scan angle $T_x b$ for H plane scan with $a/\lambda = b/\lambda = 0.5714$, $\epsilon = 3.0625$, $d_\epsilon = 0.5\lambda_\epsilon$.

transmission coefficients of the main beam and the grating lobe respectively, then

$$| R |^2 + | T_0 |^2 = 1 \quad \text{for} \quad 0 \leqq T_x b \leqq 2\pi\left(1 - \frac{b}{\lambda}\right)$$

$$| R |^2 + | T_0 |^2 + | T_1 |^2 = 1 \quad \text{for} \quad 2\pi\left(1 - \frac{b}{\lambda}\right) \leqq T_x b \leqq \pi.$$

Clearly, T_1 has significance as a transmission coefficient only in the scan range $2\pi(1 - b/\lambda) \leqq T_x b \leqq \pi$.

The graph of $| T_0 |$ shows a sharp dip at the scan angle of $T_x = 70°$, at which the reflection coefficient attains its peak value of one. Notice that the phase of T_0 exhibits a discontinuity of 180° at this scan angle. This is so because both the real and imaginary parts of T_0 go through zero and then change sign as the beam is scanned past this scan angle. This appears to indicate that $| T_0 |$ does go to zero rather than approach zero, or equivalently, that $| R |$ actually attains the value one. The significance of the difference between $| R |$ approaching one and $| R |$ actually attaining one lies in whether the match of an array can be improved by network compensation. Moreover, there is an intimate connection between the fact that $| R | = 1$ and the surface wave propagation along a plane corrugated structure. We discuss this in detail in Section IV).

Another point which might be of interest is that T_0 is the radiation pattern in the angular range $0 \leqq \theta \leqq \sin^{-1}(\lambda/2b)$, when a single element is excited with the rest of the elements terminated in the characteristic impedances.[9] The radiation pattern for the remaining angular range $\sin^{-1}(\lambda/2b) \leqq \theta \leqq \pi/2$ may be obtained from the curve of T_1 in the scan range $2\pi(1 - b/\lambda) \leqq T_x b \leqq \pi$, reflected with respect to the $T_x b = \pi$ axis.

3.3 *E Plane Scan Results*

The incident wave in the E plane scan is a TEM wave with the electric field polarized in the direction normal to the waveguide walls. Figs. 7 and 8 give the results for both the amplitudes and phases of the reflection coefficients as a function of scan. The set of parameters used for obtaining these results is: $d/\lambda = 0.5714$, $c/d = 0.85$. The array is covered with a single layer of dielectric material flush with the array aperture. A dielectric constant of $\epsilon = 3.0625$ is chosen for the same reason as for the H plane, namely to have one surface wavelike space harmonic present over as wide a scan angle as possible. Relatively thick waveguide walls are used in this case in order that the waveguides support only the dominant TEM mode, because the element spacing is larger than $\lambda/2$.

From the numerical data we may observe that, in the absence of a dielectric material, the reflection coefficient is relatively flat over a large range of scan angles, except in the vicinity of the grating lobe formation angle (in this case $T_y d = 154°$), at which we find a sharp

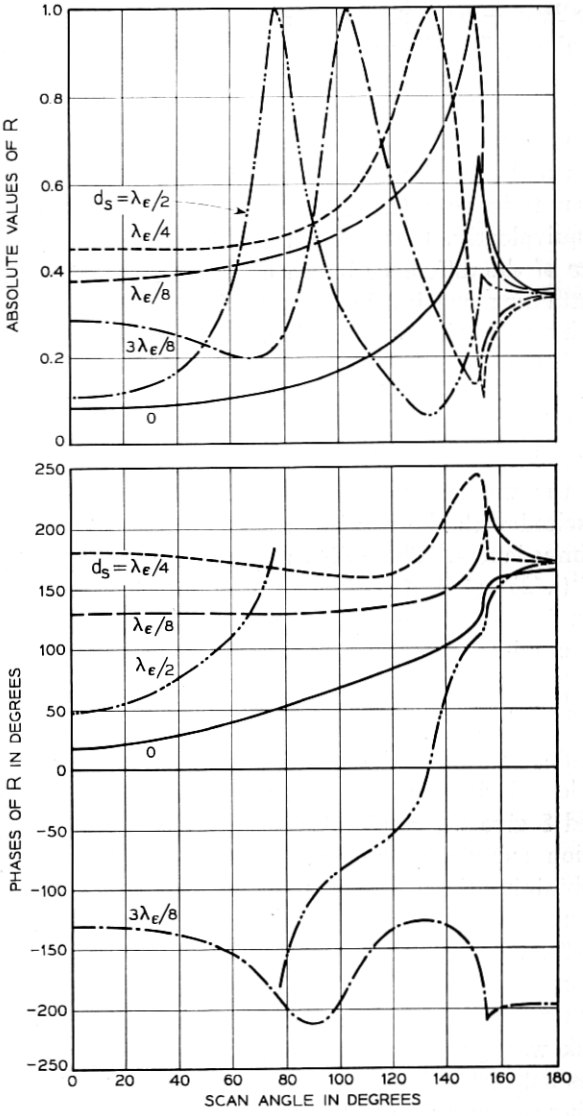

Fig. 7 — Reflection coefficient R vs scan angle $T_y d$ for E plane scan with $d/\lambda = 0.5714$, $c/d = 0.85$ and $\epsilon = 3.0625$.

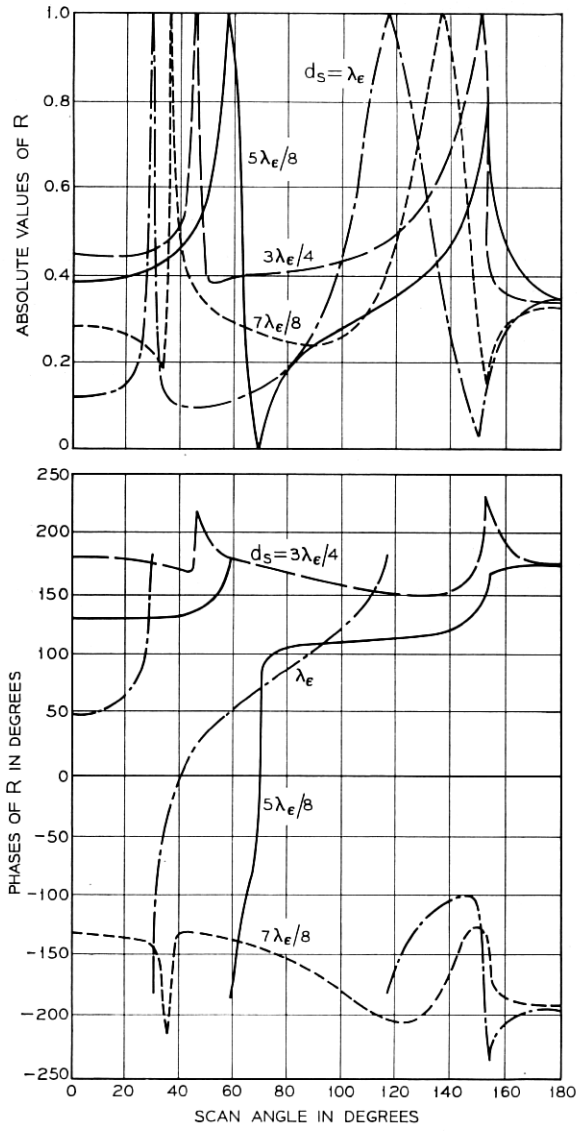

Fig. 8 — Reflection coefficient R vs scan angle $T_y d$ for E plane scan with $d/\lambda = 0.5714$, $c/d = 0.85$ and $\epsilon = 3.0625$.

peak. This is in marked contrast with the H plane scan case (see Fig. 4). The peak value does not reach one, however. When a dielectric sheath of thickness $\lambda_\epsilon/8$ is used to cover the array, the effect is to raise the level of reflection almost uniformly over all the scan angles. In particular, the peak which occurs at the grating lobe formation angle is seen to reach a value of unity. Although not presented here, the results for thinner dielectric sheaths show similar tendencies with the exception that the peak values are not necessarily unity. While the position for the appearance of the resonant peaks remains practically unchanged when the dielectric slab is relatively thin, it does start to shift toward the broadside direction as the thickness is increased beyond a critical value of about $\lambda_\epsilon/4$. A further thickening of the dielectric sheath eventually leads to the emergence of multiple resonant peaks.

3.4 *Quasi-E Plane Scan Results*

A quasi-E plane scan is a scan in which the fields have a sinusoidal variation in the direction perpendicular to the plane of scanning.[4] The reason for considering such a scan condition is that it enables us to simplify a vector three dimensional problem for a planar array to a scalar two dimensional one.

The z-directed propagation constants of the exterior modes for this case are given by

$$\beta_m = \sqrt{k^2\epsilon - \left(\frac{\pi}{b}\right)^2 - \left(\frac{2m\pi}{d} + T_y\right)^2}.$$

From this expression, it is easy to show that when $m < d\sqrt{\epsilon - (\lambda/2b)^2}/\lambda < (m + 1/2)$, there will be $(2m + 1)$ modes propagating for

$$0 \leqq T_y d \leqq 2\pi[d\sqrt{\epsilon - (\lambda/2b)^2}/\lambda - m]$$

and $2m$ modes for

$$2\pi[d\sqrt{\epsilon - (\lambda/2b)^2}/\lambda - m] \leqq T_y d \leqq \pi.$$

If $(m + 1/2) < d\sqrt{\epsilon - (\lambda/2b)^2}/\lambda < (m + 1)$, on the other hand, the number of propagating modes will increase from $(2m + 1)$ to $(2m + 2)$ as the scan angle is steered through the angle of transition $T_y d = 2\pi[m + 1 - d\sqrt{\epsilon - (\lambda/2b)^2}/\lambda]$.

With the parameters of the array chosen to be $a/\lambda = b/\lambda = 0.5714$, $c/d = 0.937$, the array radiates one beam in $0 \leqq T_y d \leqq T_{y_c} d = (2\pi d/\lambda) \cdot [1 - (\lambda/2a)^2]^{\frac{1}{2}}$, and no beam in $T_{y_c} d \leqq T_y d \leqq \pi$. Fig. 9 shows some

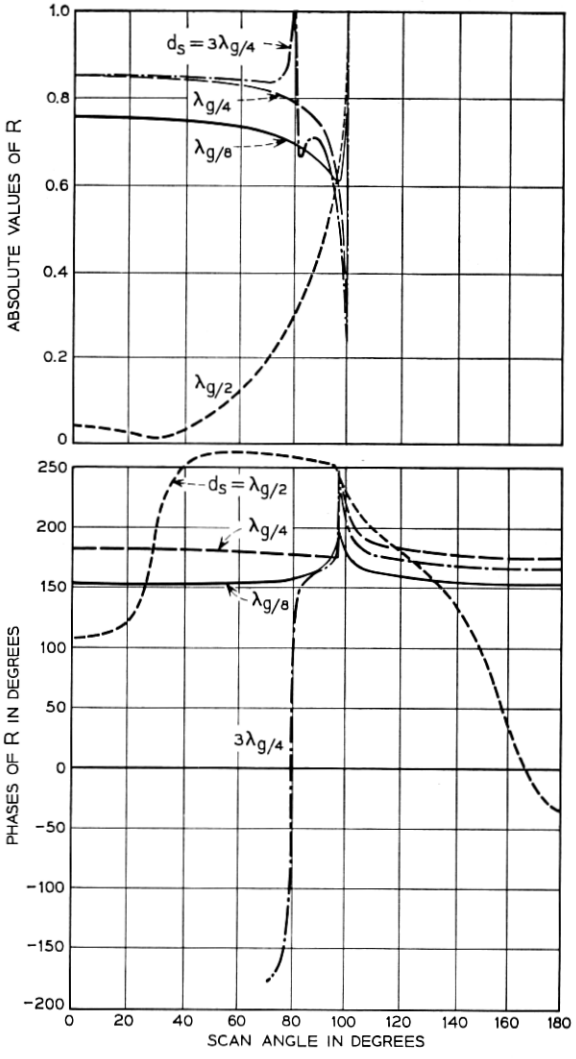

Fig. 9 — Reflection coefficient R vs scan angle $T_y d$ for quasi-E plane scan with $b/\lambda = d/\lambda = 0.5714$, $c/d = 0.937$, $\epsilon = 3.825$.

results of the reflection coefficient for this array when it is covered by a dielectric sheath with dielectric constant 3.835. The choice of this relatively large value of dielectric constant is again dictated by the interest in making as large a range of scan angle as possible for a mode in the region outside the waveguides to have surface wavelike behavior.

From the results for both the H plane and E plane scans as we already discussed, it might be anticipated that a resonant peak would be encountered with a relatively thin dielectric slab. The actual calculation, however, shows that this is not so. In fact, the reflection coefficient starts to show sharp peaks only when the slab thickness exceeds $3\lambda_g/4$, where

$$\lambda_g = \lambda_\epsilon / \sqrt{1 - (\lambda_\epsilon/2b)^2}.$$

Moreover, even when a resonant peak is present, the reflection coefficient as a function of scan is usually quite flat except near the scan angle at which the resonant peak appears.

3.5 *Effects of the Size of the Radiating Aperture*

So far, we have presented results for the situation where the element spacing and the dielectric constant were kept constant while the thickness of the dielectric sheath was varied. We studied the effects of the sheath thickness on the location of the resonant peak in some detail under these conditions.

Now let us look at some data showing the effect of the waveguide wall thickness. Fig. 10 shows both the amplitude and phase of the reflection coefficient as functions of the scan angle for an array which is scanned in the E plane and is covered by a single dielectric sheath. We obtained the results with fixed values for the element spacing $b/\lambda = 0.5714$, a dielectric constant of the sheath $\epsilon = 3.0625$, and its thickness $d_s = 0.5\ \lambda_\epsilon$. However, the waveguide wall thickness (or equivalently, the size of the radiating aperture) is varied over a wide range. It is evident from the graphs in Fig. 10 that the size of the radiating aperture has substantial effects on the reflection coefficient. The scan angle for the appearance of the resonant peak is shifted toward the broadside direction as the aperture decreases. Similar shift in the scan angle for the resonant peak has also been observed in the case of the H plane scan. Moreover, loading the waveguides with a dielectric material also causes similar effects. It is apparent that the resonance phenomenon is strongly dependent on the aperture impedance which is a function of the array parameters.

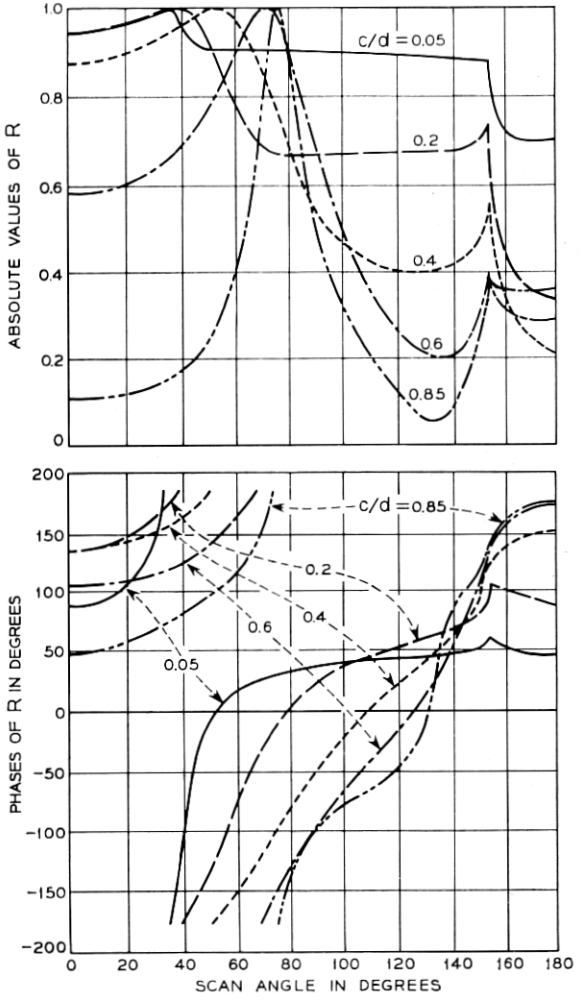

Fig. 10 — Effects of radiating aperture size (E plane scan, $d/\lambda = 0.5714$, $\epsilon = 3.0625$, $d_s = 0.5\lambda_\epsilon$).

3.6 *Thin Sheath Results*

The results presented earlier indicate that when a dielectric slab thicker than $\lambda_\epsilon/4$ is used to cover an array, an important effect is manifested by the appearance of sharp resonant peaks in the reflection coefficient. Such resonances may be avoided if thin dielectric

sheaths are used. A thin dielectric sheath covered array for H plane scanning has these dimensions: $a/\lambda = b/\lambda = 0.5714$, and the dielectric slab has a fixed thickness $d_s = \lambda/16$. We obtained the results for dielectric constants ranging from 1.25 to 3. As the graphs in Fig. 11 show, even though it does not cause "resonance," a thin dielectric slab does have a considerable effect on the array match characteristics. This is true even when the dielectric constant is close to one. In fact, in the example shown here for $\epsilon = 1.25$, the reflection coefficient seems to have a larger variation than that of an uncovered array. However, by varying the dielectric constant, and perhaps also the thickness of the slab (as long as the slab is thin), it is possible to obtain a suitable combination of these two parameters and thus achieve a flat response in both amplitude and phase of the reflection coefficient at a single frequency. Such a possibility has been demonstrated previously.[1] The significance of this possibility is that a thin dielectric slab may be used as an effective means for the wide angle match of an array over a narrow frequency band.

IV. DISCUSSIONS AND CONCLUSIONS

We have shown the effects of a dielectric slab on the radiation characteristics of a phased array. One outstanding feature of the substantial changes which the dielectric slab brings to array performance is the appearance of resonance peaks in the reflection coefficient of the array at certain scan angles. This phenomenon is caused by surface-wavelike space harmonics at the interface between the dielectric and free space.

When the fields in the free space region are expanded into a generalized Fourier series according to the Floquet theorem, each space harmonic may be viewed as homogeneous or inhomogeneous plane waves, depending on whether it is propagating or evanescent. In the absence of a secondary boundary at $z = d_s$ introduced by the dielectric slab, the plane waves generated at the array aperture either propagate away from it if they are homogeneous, or decay away if inhomogeneous.

When an air-dielectric interface is introduced at $z = d_s$, it causes each space harmonic generated at the aperture to be reflected and refracted upon encountering the interface as it travels away from the aperture. Naturally, only wave modes of the propagating type are significantly affected, because those of the evanescent type are usually rapidly attenuated away from the aperture. Furthermore,

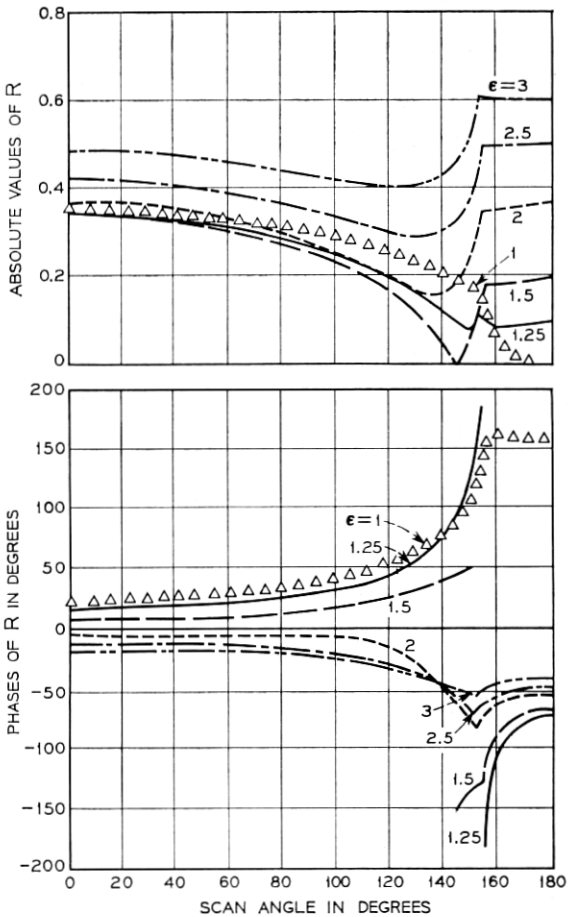

Fig. 11 — Reflection coefficient R vs scan angle $T_x b$ for an array covered with a thin dielectric slab (H plane scan, $a/\lambda = b/\lambda = 0.5714$, $d_s = \lambda/16$).

modes which exhibit a surface-wavelike field distribution suffer total reflection at the interface. The energy reflected from the interface is returned to the aperture as a wave incident to the array from the exterior region, and is scattered there.

In the presence of a dielectric sheath, there usually exists a range of scan angles over which there are two or more propagating modes inside the dielectric while only one propagating mode is present in the free space region. Under such circumstances, the two propagating

modes inside the dielectric interact as they are multiply-scattered at the array aperture. The degree of interaction depends on the various array parameters as well as the scan angle. It is then possible that, given a suitable set of parameters, the multiple scatterings between the two interfaces might lead to a situation in which a large reflection is generated at certain scan angles. The numerical examples in Section III indicate that the reflections can be so high as to reach unity for all practical purposes. In fact, it has been inferred from the numerical results for the transmission coefficient that the reflection can indeed reach the value one exactly.

4.1 *Relation with a Corrugated Structure*

The fact that the modulus of the reflection coefficient can attain exactly the value of unity assumes some special significance. For when this happens, inside the waveguides at a distance away from the array aperture such that all the evanescent modes are sufficiently attenuated, the incident and reflected waves combine to form a pure standing wave. This implies that the tangential electric and magnetic fields alternatively go through zero at one half guide wavelength intervals. Specifically, by writing $R = e^{j\varphi}$, the resultant tangential electric field under these conditions may be expressed as

$$\mathcal{E}_y(x, z) = -2jz_1 e^{j\varphi/2} \sin(\alpha_1 z - \varphi/2).$$

Hence, for $z = -L_n$ such that $(\alpha_1 L_n + \varphi/2) = n\pi$, or equivalently $L_n = (n\pi - \varphi/2)/\alpha_1$, the tangential electric field vanishes. As a consequence, electric conductors may be introduced at these positions without disturbing the field distributions of the entire system. When this is done, however, the array is then transformed into a corrugated structure which is completely isolated from the source region. The solution for the aperture fields obtained under these situations may then be regarded as the solution of a surface wave which propagates along a corrugated structure.

There are two aspects of this conclusion which deserve further comments. A corrugated surface has long been known as a structure which is capable of supporting surface waves. The characteristics of such a system are that it supports only the TM type surface wave, relative to the direction of propagation, in the *absence* of a dielectric material and that the period of corrugation be less than a half free space wavelength in order for the wave to propagate. Moreover, there is some requirement in regard to the depth of the corrugation for the surface to be properly reactive.

The introduction of a dielectric sheath above the array aperture or corrugated surface produces two significant effects. One is to enable a surface wave to propagate in the TE mode, corresponding to the case of H plane scan, as well as in the TM mode. The other is that the surface wave propagation is possible even though the period of corrugation is larger than a half free-space wavelength. It is important to observe that when the corrugation period is larger than a half wavelength, the zeroth space harmonic of the fields outside the corrugation is a propagating mode. Therefore, it is necessary for the modal coefficient of this mode to be identically zero in order for the fields to conform to that of a surface wave. The results presented in this calculation indicate that indeed this is the case.

4.2 *Determination of the Location of the Resonant Peak*

The scan angles at which resonant peaks appear may be determined accurately by the transverse resonant method when the radiating aperture is small. This situation applies readily to the case of the E plan scan. In this method, the sum of impedances looking towards the positive and negative z directions at some reference plane is set equal to zero, thus yielding a characteristic equation. It is convenient to use the array aperture as the reference plane. When the radiation aperture is small in comparison to the size of a periodic cell, the "average" impedance looking toward the array side is almost zero. The impedance looking away from the aperture may be approximated by that of the lowest order mode, in this case the (-1)st space harmonics. The impedance of this mode is given by

$$Z'_{-1} = Z^D_{-1} \frac{Z^0_{-1} - jZ^D_{-1} \tan \beta_{-1} d_s}{Z^D_{-1} - jZ^0_{-1} \tan \beta_{-1} d_s}.$$

By setting this expression to zero and using the appropriate modal impedances, we find

$$\epsilon\gamma_{-1} = j\beta_{-1} \tan \beta_{-1} d_s .$$

When this equation is used to determine the scan angle for the appearance of the resonant peak, it is found that excellent agreement with actual calculation is obtainable for aperture size up to 10 percent of the size of the periodic cell. For larger aperture sizes, the agreement gradually becomes poorer. This is because the impedance looking toward the waveguide side no longer remains negligibly small. It appears at this time that an accurate determination of the scan angle for resonant peaks under such conditions is best carried out by

solving the boundary value problem directly. Fortunately, this is a relatively easy task nowadays with the help of high speed electronic computers.

4.3 *Array Match*

The numerical results obtained so far have revealed that the occurrence of sharp resonant peaks is associated with rather thick dielectric sheaths, and such resonance may be avoided by using thin sheaths. Thus, dielectric covering of an array is still a useful tool for the protection of the array from its environment. More importantly, the scan (or incident angle) dependent reflectivity of dielectric slabs may be utilized to advantage in improving the match performance of an array. The feasibility of this desirable feature has been demonstrated by extensive data presented herein and in [1]. It has also been suggested by other workers.[8, 10] Although, based on the calculated results, the improvement in array match by a thin dielectric sheath is obtainable at the expense of a higher frequency sensitivity, it seems possible to achieve a broadband compensation by using multiple thin sheaths. Further work is being carried out along this line, and the results will be reported at a later date.

REFERENCES

1. Galindo, V. and Wu, C. P., Dielectric Loaded and Covered Rectangular Waveguide Phased Arrays, presented at International Symposium on Antennas and Propagation, Palo Alto, California, December 1966.
2. Galindo, V. and Wu, C. P., Numerical Solutions for an Infinite Phased Array of Rectangular Waveguides with Thick Walls, IEEE Trans. Antennas and Propagation, *AP-14,* March 1966, pp. 149–158.
3. See, for example, J. R. Wait, *Electromagnetic Waves in Stratified Media,* The Macmillan Co., New York, 1962, Chapter 2.
4. Wu, C. P. and Galindo, V., Properties of a Phased Array of Rectangular Waveguides with Thin Walls, IEEE Trans. Antennas and Propagation, *AP-14,* March 1966, pp. 163–172.
5. Hildebrand, F. B., *Methods of Applied Mathematics,* Prentice-Hall, Inc., New York, 1954, pp. 451–452.
6. Kantorovitch, L. V. and Krylov, V. I., *Approximate Methods of Higher Analysis,* Interscience Publishers, New York, 1958.
7. *Waveguide Handbook,* N. Marcuvitz, ed., Radiation Laboratory, Series 10, McGraw-Hill Book Co., New York, 1950.
8. Lee, S. W., Impedance Matching of an Infinite Phased Array by Dielectric Sheets, Electronics Letters, *2,* October 1966, pp. 366–368.
9. Galindo, V. and Wu, C. P., The Relation Between the Far-Zone Pattern of the Singly Excited Element and the Transmission Coefficient of the Principal Lobe in an Infinite Array, IEEE Trans. Antennas and Propagation, *AP-14,* May 1966, pp. 397–398.
10. Magill, E. G. and Wheeler, H. A., Wide Angle Impedance Matching of a Planar Array Antenna by a Dielectric Sheet, IEEE Trans. Antennas and Propagation, *AP-14,* January 1966, pp. 49–53.
11. Collin, R. E., *Field Theory of Guided Waves,* McGraw-Hill Book Co., New York, 1960, Chapter 8.